

# SYNTHETIC APERTURE RADAR IMAGING FROM TRUNCATED DATA

Alessandra Budillon<sup>(1)</sup>, Vito Pascazio<sup>(1)</sup>, Daniele Pisa<sup>(1)</sup>, Gilda Schirinzi<sup>(2)</sup>

<sup>(1)</sup> Dipartimento per le Tecnologie - Università di Napoli “Parthenope”  
via Acton 38, 80133 Napoli (Italy), ☎ +39 081 5513976, Fax +39 081 5512884  
email: {alessandra.budillon,vito.pascazio}@uniparthenope.it

<sup>(2)</sup> DAEIMI - Università di Cassino  
via Di Biasio 43, 03043 Cassino (Italy), ☎ +39 0776 2993654, Fax +39 0776 310812  
email: schirinzi@unicas.it

## ABSTRACT

In this paper a new approach to synthetic aperture radar (SAR) data processing, is presented. The method properly takes into account the spatial truncation of the data in the azimuth direction, due to the finite recording frame. It allows an enlargement of the well focused area, assuring lower reconstruction error, respect to conventional processing techniques. The good performance of the method is demonstrated through reconstructions from simulated data, putting emphasis on the well focused signals.

## 1. INTRODUCTION

Synthetic Aperture Radar (SAR) is a microwave imaging system carried out by a moving platform emitting and then receiving pulses at a given pulse repetition frequency. Collected data are then coherently processed to generate high resolution images of the illuminated scene. The received data are related to the reflectivity function to be estimated through a space varying convolution [1], truncated in the motion direction of the platform. SAR image focusing amounts to search for a finite resolution estimate of the ground reflectivity function, i. e. belonging to a finite dimensional space, starting from the knowledge of the received signal acquired over a finite recording interval. Then, it can be stated as a deconvolution problem from truncated data. This is an ill posed problem, that is usually met in the field of image restoration [2]. Conventional processing techniques [1], that make use of a matched filter and operate in the Fourier domain, implicitly regularize the problem by forcing to zero the data outside the recording interval. For this reason, only a part of the resulting image, of smaller dimension respect to the data dimension, is well focused. This paper describes a new approach to SAR data processing that explicitly takes into account the data truncation. Moreover, the method allows the regularization of the problem introducing a convenient representation of the signal to be estimated involving a lower number of unknowns.

The success of the method is demonstrated through reconstructions from simulated data, showing a noticeable enlargement of the well focused area and an improvement of

fidelity respect to conventional approaches. Moreover it enables the incorporation of possible *a priori* information on the scene directly in the reconstruction process. This features can be conveniently exploited in many applications, such as edge detection and image segmentation and image classification.

## 2. STATEMENT OF THE PROBLEM

In a radar system the (noise-free) signal received after back-scattering can be described by the discrete linear convolution:

$$\mathbf{y} = \mathbf{h} * \mathbf{x}, \quad (1)$$

where  $\mathbf{x}=[x_1 \ x_2 \ \dots \ x_M]^T$  is the discretized reflectivity of the ground,  $\mathbf{h}=[h_1 \ h_2 \ \dots \ h_P]^T$  is the system impulse response, and  $\mathbf{y}=[y_1 \ y_2 \ \dots \ y_N]^T$ , with  $N=M+P-1$ , is the radar received signal.

Note that, while the dimension  $P$  of the impulse response is limited by the system characteristics (for instance by the antenna angular aperture), the dimension of the reflectivity vector is limited by the acquisition interval of the radar receiver, so that its value  $M$  is much larger than  $P$ . Moreover, we refer to one-dimensional signals for simplicity, but our method it can be easily generalized to the SAR 2-D signals (raw data). The discrete model (1) can be also written, exploiting the convolution theorem, in the following way:

$$\mathbf{y} = F^{-1} [F(\mathbf{h}) \odot F(\mathbf{x})], \quad (2)$$

where  $F$  is the discrete Fourier Transform (DFT),  $F^{-1}$  is the inverse discrete Fourier Transform (IDFT), and  $\odot$  is the Hadamard product, i.e. the vector element-wise product. Frequency domain model (2) and time domain (1) provide the same result (the linear convolution) if both  $\mathbf{h}$  and  $\mathbf{x}$  are zero-padded (through the zero-padding matrix  $\mathbf{Z}$ ) to  $N$ -length vectors before performing DFT. It is easy to verify that the zero-padding matrix  $\mathbf{Z}$ , when applied to a  $M$ -order vector to provide a  $N$ -vector one, is given by:

$$\mathbf{Z} = \begin{bmatrix} 1 & 0 & 0 & \cdots & 0 \\ 0 & 1 & 0 & \cdots & 0 \\ 0 & 0 & 1 & \cdots & 0 \\ \vdots & \vdots & \ddots & \ddots & \vdots \\ 0 & 0 & 0 & \cdots & 1 \\ 0 & 0 & 0 & \cdots & 0 \\ \vdots & \vdots & \ddots & \ddots & \vdots \\ 0 & 0 & 0 & \cdots & 0 \end{bmatrix} = \begin{bmatrix} \mathbf{I}_{M \times M} \\ \mathbf{0}_{(N-M) \times M} \end{bmatrix}, \quad (3)$$

where  $\mathbf{I}_{M \times M}$  is the  $M$ -order identity matrix, and  $\mathbf{0}_{(N-M) \times M}$  is a  $[(N-M) \times M]$ -order null matrix.

Eq. (2) becomes:

$$\mathbf{y} = \mathbf{F}^{-1} [\mathbf{F}(\mathbf{Z} \mathbf{h}) \odot \mathbf{F}(\mathbf{Z} \mathbf{x})]. \quad (4)$$

Since  $F$  can be written as a matrix operator  $\mathbf{F}$  [3], the  $N$ -th-order vector of the DFT of  $\mathbf{h}$  can be written as the following matrix vector product:

$$\tilde{\mathbf{h}} = \mathbf{F}(\mathbf{Z} \mathbf{h}) = \mathbf{F} \mathbf{Z} \mathbf{h}. \quad (5)$$

Analogously, the IDFT  $F^{-1}$  can be expressed in matrix form as the complex conjugate of  $\mathbf{F}$ .

If we introduce a new diagonal matrix  $\mathbf{D}$ , defined as

$$\mathbf{D} = \begin{bmatrix} \tilde{h}(0) & 0 & \cdots & 0 \\ 0 & \tilde{h}(1) & \cdots & 0 \\ \vdots & \vdots & \ddots & \vdots \\ 0 & 0 & \cdots & \tilde{h}(N-1) \end{bmatrix}, \quad (6)$$

where  $\tilde{h}(n)$  are the elements of vector  $\tilde{\mathbf{h}}$ , model (2) can be written in the following way:

$$\mathbf{y} = \mathbf{F}^{-1} \mathbf{D} \mathbf{F} \mathbf{Z} \mathbf{x}. \quad (7)$$

Models (7) and (1) are perfectly equivalent: when they are applied to the same reflectivity  $\mathbf{x}$ , they provide the same received signal  $\mathbf{y}$ .

The actual world model is given by:

$$\begin{aligned} \mathbf{y} &= \mathbf{h} * \mathbf{x} + \mathbf{n} = \\ &= \mathbf{F}^{-1} \mathbf{D} \mathbf{F} \mathbf{Z} \mathbf{x} + \mathbf{n}, \end{aligned} \quad (8)$$

where  $\mathbf{n}$  represent additive white Gaussian noise (AWGN). In practise, the SAR received data used to form the SAR images are a subset of  $\mathbf{y}$ . In Fig. 1 it is shown such subset is taken by spatial truncation of  $\mathbf{y}$  along the flight direction.

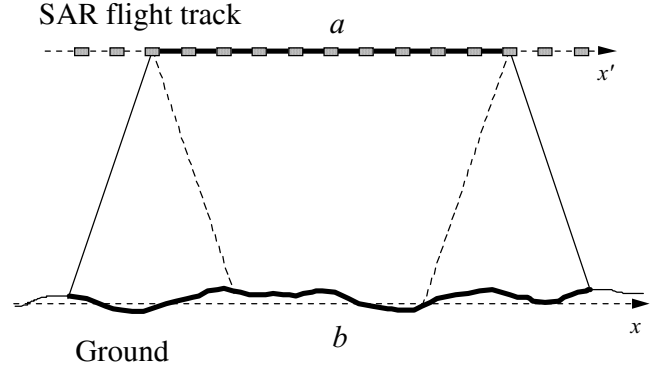


Figure 1: Acquisition of a SAR raw data subset.

If we suppose to extract  $K$  samples of the  $N$  samples of the received data vector  $\mathbf{y}$ , such truncation can be explicitly taken into account in the received data model by introducing a truncation operator:

$$\underline{\mathbf{y}}_t = \underbrace{\mathbf{T} \mathbf{F}^{-1} \mathbf{D} \mathbf{F} \mathbf{Z}}_{K \times M} \underline{\mathbf{x}} + \underline{\mathbf{n}} \quad (9)$$

where  $\mathbf{T}$  is the truncation  $[K \times N]$ -order matrix defined as:

$$\begin{aligned} \mathbf{T} &= \begin{bmatrix} 0 & \cdots & 0 & 1 & 0 & \cdots & 0 & 0 & 0 & \cdots & 0 \\ 0 & \cdots & 0 & 0 & 1 & \cdots & 0 & 0 & 0 & \cdots & 0 \\ \vdots & \ddots & \vdots & \vdots & \vdots & \ddots & \vdots & \vdots & \vdots & \ddots & \vdots \\ 0 & \cdots & 0 & 0 & 0 & \cdots & 1 & 0 & 0 & \cdots & 0 \\ 0 & \cdots & 0 & 0 & 0 & \cdots & 0 & 1 & 0 & \cdots & 0 \end{bmatrix} \quad (10) \\ &= \begin{bmatrix} \mathbf{0}_{K \times N_1} & \mathbf{I}_{K \times K} & \mathbf{0}_{K \times N_2} \end{bmatrix}, \end{aligned}$$

$N_1 + K + N_2 = N$ , and  $\mathbf{I}$  and  $\mathbf{0}$  can be interpreted extending previous definitions.

### 3. IMAGE FORMATION BY TRUNCATED DATA

In Fig. 1 it is shown that the received data are recorded over the finite space interval of length  $a$ , and contain information on the ground reflectivity pattern of extension  $b$ , always greater than  $a$ .

By adopting the same sampling step for  $\mathbf{y}_t$  and  $\mathbf{x}$ , as usually done, it will result that  $\mathbf{x}$  ( $M$  unknown of the problem) exhibits more samples than  $\mathbf{y}_t$  ( $K$  available data):  $M \geq K$ . Then, it has to be considered that when  $K$  data are assigned, at most the same number of unknown parameters can be univocally determined. Such under-determined mapping cannot be inverted unless regularization is adopted.

The standard data processing of model (9) is implicitly regularized [1], because it allows to get more image (unknown) samples than (non trivial) data samples by forcing to zero the data that are outside the recording interval. It suffices to add zero samples to  $\mathbf{y}_t$  till the  $M$ -th one (a new zero padding matrix  $\mathbf{Z}_t$ ), and to perform the mapping inversion (basically a deconvolution):

$$\hat{\mathbf{x}} = \left( \mathbf{Z}_1 \mathbf{T} \mathbf{F}^{-1} \mathbf{D} \mathbf{F} \mathbf{Z} \right)^{-1} \mathbf{Z}_1 \mathbf{y}_t. \quad (11)$$

The previous solution procedure is equivalent to search for an estimate  $\hat{\mathbf{x}}$  such that its convolution with  $\mathbf{h}$  will simultaneously matches the received signal in the part where the data are available, and matches zero in the part where the data have been forced to zero by  $\mathbf{Z}_1$ . This solution will necessarily be different from the actual ground reflectivity function that matches the recorded received signal and does not produce a signal equal to zero outside the recording interval. The resulting estimation will exhibit a good accuracy only in the central part of the whole computed reflectivity, namely a zone formed by  $(K-P+1)$  signal samples.

The new procedure proposed in this paper amounts to take into proper account the nature of mapping (9), in particular its truncation, its under-determined nature, and the nature of noise. As far as the under-determined nature of the mapping is concerned, in order to restore the equality between data and unknowns, we introduce the following transformation operator:

$$\begin{aligned} \mathbf{x} &= \mathbf{P} \mathbf{x}_l, \\ \mathbf{P} : \mathbb{C}^K &\rightarrow \mathbb{C}^M. \end{aligned} \quad (12)$$

$\mathbf{P}$  is a mapping from a lower dimensional space to a higher dimensional one, and it typically consists of an interpolation (Fourier oversampling, spline-based, wavelets-based, etc.). If such operator is chosen properly, it results that the model can be well approximated by:

$$\mathbf{y}_t \cong \mathbf{T} \mathbf{F}^{-1} \mathbf{D} \mathbf{F} \mathbf{Z} \mathbf{P} \mathbf{x}_l + \mathbf{n} = \mathbf{A} \mathbf{x}_l + \mathbf{n}, \quad (13)$$

where  $\mathbf{A} \triangleq \mathbf{T} \mathbf{F}^{-1} \mathbf{D} \mathbf{F} \mathbf{Z} \mathbf{P}$ . Now, exploiting the linear nature of mapping (13), and the AWG nature of noise, an ML solution in the complex field [3] can be adopted:

$$\begin{aligned} \hat{\mathbf{x}}_l &= \left( \mathbf{A}^H \mathbf{A} \right)^{-1} \mathbf{A}^H \mathbf{y}_t \\ &= \left( \mathbf{P}^H \mathbf{Z}^T \mathbf{F}^{-1} \mathbf{D}^H \mathbf{F} \mathbf{T}^T \mathbf{T} \mathbf{F}^{-1} \mathbf{D} \mathbf{F} \mathbf{Z} \mathbf{P} \right)^{-1} \mathbf{P}^H \mathbf{Z}^T \mathbf{F}^{-1} \mathbf{D}^H \mathbf{F} \mathbf{T}^T \mathbf{y}_t \end{aligned} \quad (14)$$

where superscript ‘‘H’’ denotes ‘‘Hermitian’’ matrices, and ‘‘T’’ denotes ‘‘transpose’’ matrices.

It is easy to note that transposition of above defined truncation  $\mathbf{T}$  is equivalent to a particular zero-padding, where part of the zeros are positioned at left, and part at right of the sequence, and transposition of above defined (3) zero-padding  $\mathbf{Z}$  is equivalent to a particular truncation, where truncation is made on the right part of the sequence.

The processing scheme (14) consist essentially of zero padding and truncation operators (no time consuming), of element-wise products (no time consuming), of Fourier transforms and interpolation operators, plus a matrix inversion. These last operations requires computational times. In particular, the formal inversion of the square matrix  $\mathbf{A}^H \mathbf{A}$  can be in practice a prohibitive task due to the huge dimension of

the involved actual vectors. In that case the inversion can be performed by making resort to iterative schemes determining the MSE solution:

$$\hat{\mathbf{x}}_l = \arg \min_{\mathbf{x}} \phi(\mathbf{x}), \quad \phi(\mathbf{x}) = \|\mathbf{A} \mathbf{x}_l - \mathbf{y}_t\|^2. \quad (15)$$

In order to minimize  $\phi(\mathbf{x}_l)$  we can adopt a conjugate gradient based method [4]. Due to the huge amount of data, it is convenient to evaluate the formal expression of the gradient, that is given by:

$$\nabla \phi = 2 \mathbf{A}^H [\mathbf{A} \mathbf{x}_l - \mathbf{y}_t], \quad (16)$$

and, the expression of the coefficients of the quadratic function  $\phi(\mathbf{x}_l + \lambda \Delta \mathbf{x}_l) = a \lambda^2 + b \lambda + c$ , along which the minimization line is performed step by step:

$$a = \|\mathbf{A} \mathbf{x}_l\|^2, \quad b = 2 \Re \langle \mathbf{A} \mathbf{x}_l, \mathbf{A} \mathbf{x}_l \rangle, \quad c = \|\mathbf{A} \mathbf{x}_l - \mathbf{y}_t\|^2. \quad (17)$$

It is easy to show that the optimal step is  $\lambda_{\text{opt}} = -b/2a$ .

#### 4. NUMERICAL EXPERIMENTS AND DISCUSSION

To show the good performance of the presented method, three significant numerical experiments have been performed on simulated data.

The first experiment is related to the case of three targets, where two of them are spaced more than a full resolution cell. The radar received signal has been truncated on left sides, in such a way that the response of the right target has not been interested by truncation. A full spatial resolution is expected for the right target, and a worse resolution is expected for the left lateral targets. The resulting spatial resolution after truncation is lower than the distance between left side pixels, so that they can be still distinguish after image formation. The result of the conventional processing algorithm (11) and of the new proposed algorithm (14) are shown in Figs. 2 (top and bottom, respectively). The conventional processing is unable to recover the spatial resolution for the target positioned in the sequence portion interested by truncation. This effect is due to the presence of zero samples forced by  $\mathbf{Z}_1$  in (11), not corresponding to a true physical condition. The best theoretical resolution (better for the right target, worse for the left ones) is instead fully recovered applying the new proposed algorithm (14).

The second experiment has been proposed to test the performance with a continuous reflectivity function. The data relative to a rect-wise continuous pattern has been simulated. The radar received signal has been truncated on both sides, in such a way that the response of the central part has not been interested by truncation. The signal obtained by using conventional processing and the presented method are presented in Fig. 3 (top and bottom, respectively). The enlargement of the focused area is still evident. In particular, the reflectivity pattern reconstructed with the proposed method matches a

rect function better than the one obtained through the conventional focusing.

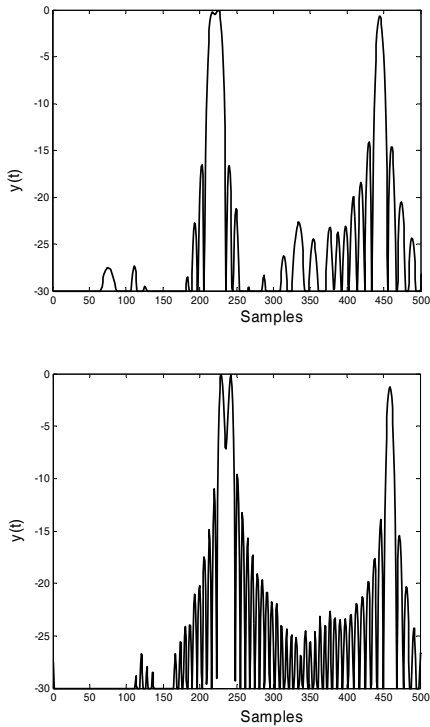


Figure 2: Three targets reflectivity reconstructed by using the conventional method (top), and the proposed method (bottom).

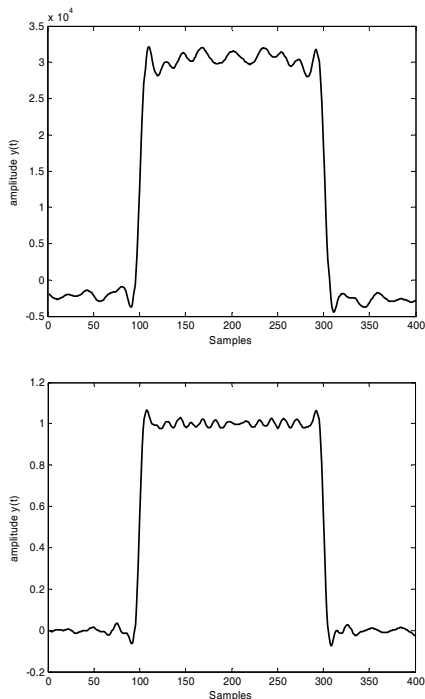


Figure 3: A rect-wise continuous reflectivity pattern reconstructed by using the conventional method (top), and proposed method (bottom).

The third experiment has been proposed to evaluate the phase-preserving performance of the proposed algorithm. The preservation of the signal phase is very important in radar imaging application. It suffices to think to SAR interferometry, and to all coherent processing applications. The data relative to a constant reflectivity amplitude pattern with a linear phase has been simulated. The radar received signal has been truncated. The reference signal phase is plotted with the solid line in Fig.4. The signal phase obtained by using conventional processing and the presented method are presented in Fig. 4 (dotted line, and dashed-dotted line, respectively).

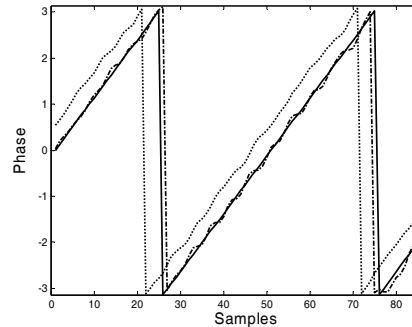


Figure 4: Reference signal phase (solid line), signal phase obtained by conventional processing (dotted line), and signal phase obtained by new proposed processing (dashed-dotted line).

In all presented numerical experiments it appears evident the quality improvements due to the application of the proposed algorithm with respect to the conventional one.

## 5. CONCLUSIONS

A new algorithm to process truncated radar data has been proposed in this paper. The proposed technique takes into proper account the present sequence truncation, and the under-determined nature of the linear model between data and unknowns. In particular, it allows to avoid the fictitious zero padding, necessary to restore the well-posedness of the problem, but devoid of physical meaning. The presented results show the effectiveness of the proposed method with respect to the results relative to the application of the conventional method.

It has to be remarked that the proposed method can be applied to all the situation where data truncation (spatial or temporal) is present.

## REFERENCES

- [1] G. Franceschetti, G. Schirinzi, "A SAR Processor Based on Two-Dimensional FFT Codes", *IEEE Trans. Aerospace Electron. Syst.*, vol. 26, pp. 356-366, 1990.
- [2] R. H. T. Bates, M. J. McDonnell, *Image Restoration and Reconstruction*, Clarendon Press, Oxford, 1986.
- [3] S. M. Kay, *Fundamentals of Statistical Signal Processing: Estimation Theory*, Prentice Hall Int. Inc., Englewood Cliffs, New Jersey, 1993.
- [4] D. G. Luenberger, *Linear and Non Linear Programming*, Addison-Wesley, 1989.